

Behind the curtain of the compartmentalization process: Exploring how xylem vessel diameter impacts vascular pathogen resistance

Jérôme Pouzoulet¹  | Philippe E. Rolshausen² | Rémi Charbois¹ | Jinliang Chen¹ | Sabine Guillaumie¹ | Nathalie Ollat¹ | Gregory A. Gambetta¹ | Chloé E. L. Delmas³ 

¹EGFV, INRAE, Bordeaux-Sciences Agro, Université Bordeaux, ISVV, Villenave d'Ornon, France

²Department of Botany and Plant Sciences, University of California, Riverside, California

³SAVE, INRAE, Bordeaux-Sciences Agro, ISVV, Villenave d'Ornon, France

Correspondence

Jérôme Pouzoulet, EGFV, INRAE, Bordeaux-Sciences Agro, Université Bordeaux, ISVV, 33882 Villenave d'Ornon, France.
Email: jerome.pouzoulet@gmail.com

Funding information

European Union Commission: Agreenskills+, Grant/Award Number: 1357; FranceAgriMer and CNIV, Grant/Award Number: 22001150-1506; Région Nouvelle-Aquitaine, Grant/Award Number: 2017-1R20209; U.S. Department of Agriculture, Grant/Award Number: 2012-51181-19954

Abstract

A key determinant of plant resistance to vascular infections lies in the ability of the host to successfully compartmentalize invaders at the xylem level. Growing evidence supports that the structural properties of the vascular system impact host vulnerability towards vascular pathogens. The aim of this study was to provide further insight into the impact of xylem vessel diameter on compartmentalization efficiency and thus vascular pathogen movement, using the interaction between *Vitis* and *Phaeoaniella chlamydospora* as a model system. We showed experimentally that an increased number of xylem vessels above 100 μm of diameter resulted in a higher mean infection level of host tissue. This benchmark was validated within and across *Vitis* genotypes. Although the ability of genotypes to restore vascular cambium integrity upon infection was highly variable, this trait did not correlate with their ability to impede pathogen movement at the xylem level. The distribution of infection severity of cuttings across the range of genotype's susceptibility suggests that a risk-based mechanism is involved. We used this experimental data to calibrate a mechanistic stochastic model of the pathogen spread and we provide evidence that the efficiency of the compartmentalization process within a given xylem vessel is a function of its diameter.

KEYWORDS

grapevine, mechanistic model, plant, tolerance, xylem anatomy

1 | INTRODUCTION

Diseases caused by vascular pathogens encompass many annual and perennial plant species and can be particularly detrimental for both agriculture and natural ecosystems (Gramaje et al., 2016; Liebhold et al., 2017; Showalter et al., 2018). As these pathogens colonize the vascular system, the xylem conductivity of the host progressively decreases due to the occlusion of vessels by tyloses and gels triggered by the host in order to compartmentalize the infection (Pearce, 1996; Yadeta & Thomma, 2013). This loss of hydraulic conductivity has negative effects on the plant and according to the extent of infection can

ultimately lead to plant death (Deyett et al., 2019; Inch & Ploetz, 2012). Because vascular pathogens reside in the wood, the use of curative management strategies are usually difficult to implement or ineffective (Aćimović, Martin, Turcotte, Meredith, & Munck, 2019; Jiménez-Díaz et al., 2011; Mondello et al., 2017). Control strategies preventing the infection can sometimes be used, but the planting of tolerant or resistant genotypes appears to be a more sustainable long-term approach (Jiménez-Díaz et al., 2011; Sniezko & Koch, 2017).

Xylem is a complex and heterogeneous tissue where the spatio-temporal organization of defences also plays a pivotal role in the ability of the host to wall-off microbial attacks (Beckman & Roberts, 1995;

Morris, Brodersen, Schwarze, & Jansen, 2016; Pearce, 1996). The CODIT model illustrates how anatomical barriers within the xylem could be used strategically to restrict the movement of pathogens (Shigo, 1984). For instance, the restriction of longitudinal movement of pathogens is principally achieved by the occlusion of xylem vessels, whereas lateral movements are mainly limited by reactions taking place within ray parenchyma (i.e., cell wall reinforcement, accumulation of antimicrobial compounds). Although investigating the dynamic aspects of host-pathogen interactions in the xylem poses practical difficulties, some observations suggested that xylem defence is established through static boundaries that might ultimately be overcome (Pearce, 1996). This implies that colonization of the host by the pathogen follows alternations of phases of stasis and active invasion. The colonization of host vasculature by wilt fungi is likely ruled in the same manner, their spread involving a series of entrapment at the vessel end and de novo colonization of functional vessels (Beckman & Roberts, 1995).

Regarding the colonization strategy adopted by vascular pathogens and the organization of defence in the wood, it can be anticipated that morphological features of the vascular system impact a host's ability to contain infections (Fradin & Thomma, 2006). The body of literature addressing these questions has mainly focused on traits that could impact the rate of the spread of pathogens and their peripheral distribution in plant organs (Beckman, Vandermolten, Mueller, & Mace, 1976; Chatelet, Matthews, & Rost, 2006; Martín, Solla, Esteban, de Palacios, & Gil, 2009; Martín, Solla, Ruiz-Villar, & Gil, 2013). The diameter and length of xylem vessels, their connectivity, and some features of bordered pits (morphology, abundance and chemical properties of the pit membrane) were proposed as factors contributing to the resistance of elm (*Ulmus minor*) and grapevine (*Vitis spp.*) towards *Ophiostoma novo-ulmi* (i.e., Dutch elm disease) and *Xylella fastidiosa* (i.e., Pierce's disease), respectively (Brodersen et al., 2013; Chatelet, Wistrom, Purcell, Rost, & Matthews, 2011; Martín et al., 2009; Solla & Gil, 2002a; Sun, Greve, & Labavitch, 2011). Recently, the density of wide diameter xylem vessels was found to correlate with the susceptibility of grapevine genotypes (*Vitis vinifera* L.) to the vascular pathogen *Phaeoaniella chlamydospora* (Pouzoulet, Scudiero, Schiavon, & Rolshausen, 2017). Numerous hypotheses have been formulated on the physiological processes linking the host vascular system to pathogen resistance. For example, the effect of vessel dimension (both diameter and length) was often attributed to changes in vessel hydraulic properties and sap velocity that would differentially assist the upward movement of fungal propagules and/or toxins (Solla & Gil, 2002a; Venturas, López, Martín, Gascó, & Gil, 2014). The loss of hydraulic function of wider vessels, due to occlusion or embolism triggered by pathogen infection, results in a greater loss of hydraulic conductance compared to narrower vessels (Newbanks, Bosch, & Zimmermann, 1983; Pérez-Donoso, Greve, Walton, Shackel, & Labavitch, 2007; Pouzoulet, Pivovarov, Santiago, & Rolshausen, 2014; Solla & Gil, 2002a). As a consequence, hosts with wider vessels could be exposed to higher risks of hydraulic failure upon infection. There is also evidence that vessel diameter (D_v , see Table 1) impacts the compartmentalization process through changing the dynamics of vessel occlusion by tyloses (Pouzoulet et al., 2017;

TABLE 1 List of abbreviations used in this manuscript and their explanations

Abbreviation	Explanation	Unit
CG	Commercial grapevine genotypes trial	—
CS	Cabernet-sauvignon	—
cv.	Cultivar	—
D_v	Xylem vessel diameter	μm
DV	Dorso-ventral sector of the grapevine stem	—
DWV	Density of wide diameter xylem vessels	Count/ mm^2
F2	F2 CS \times RGM genotypes trial	—
FDA	Fungal DNA amount (fg) per initial starting DNA (ng)	fg/ng
GA	Genetic algorithm	—
L	Lateral sector of the grapevine stem	—
L_{failure}	Length of pathogen spread once compartmentalization fails	Arbitrary length unit
NLL	Necrotic lesion length	mm
P_{failure}	Probability of compartmentalization failure	—
RMSE	Root mean square error	—

Pouzoulet, Scudiero, Schiavon, Santiago, & Rolshausen, 2019). Thus, the biological processes by which morphological features of the xylem impact host resistance are likely diverse.

The impact of the structural properties of the vascular systems on traits such as productivity and resistance to drought has been well studied, including using modelling approaches to test the validity of biological hypotheses at the vessel level (Bouda, Windt, McElrone, & Brodersen, 2019; Lauri et al., 2011; Lens et al., 2011; Mrad, Domec, Huang, Lens, & Katul, 2018; Venturas, Sperry, & Hacke, 2017). Comparatively, the impact of xylem morphology on host vulnerability to biotic attack has received little attention, despite reports supporting its involvement in several pathosystems (Martín et al., 2009; Pouzoulet et al., 2017; Sabella et al., 2019; Solla & Gil, 2002a). Here, we investigated the impact of plant vascular structure on host vulnerability using the pathogen *P. chlamydospora*/grapevine model system. We hypothesized that the susceptibility to the pathogen of a given genotype is driven by the anatomical distribution of the vessel diameter within the grapevine stem (lateral vs. dorsal-ventral [DV] sectors; Figure 1) (Brodersen et al., 2013; Pouzoulet et al., 2014; Stevenson, Matthews, & Rost, 2004). Second, we speculated that the difference in D_v density across different genotypes is a key determinant of susceptibility to fungal infection. Although this has been tested previously on a limited range of grapevine genotypes (Pouzoulet et al., 2017), our goal was to confirm the relationship between the density of wide diameter vessels and host susceptibility across a broad range of genotypes of commercial grapevine varieties (i.e., cultivars) and genotypes from an experimental *Vitis* hybrid cross.

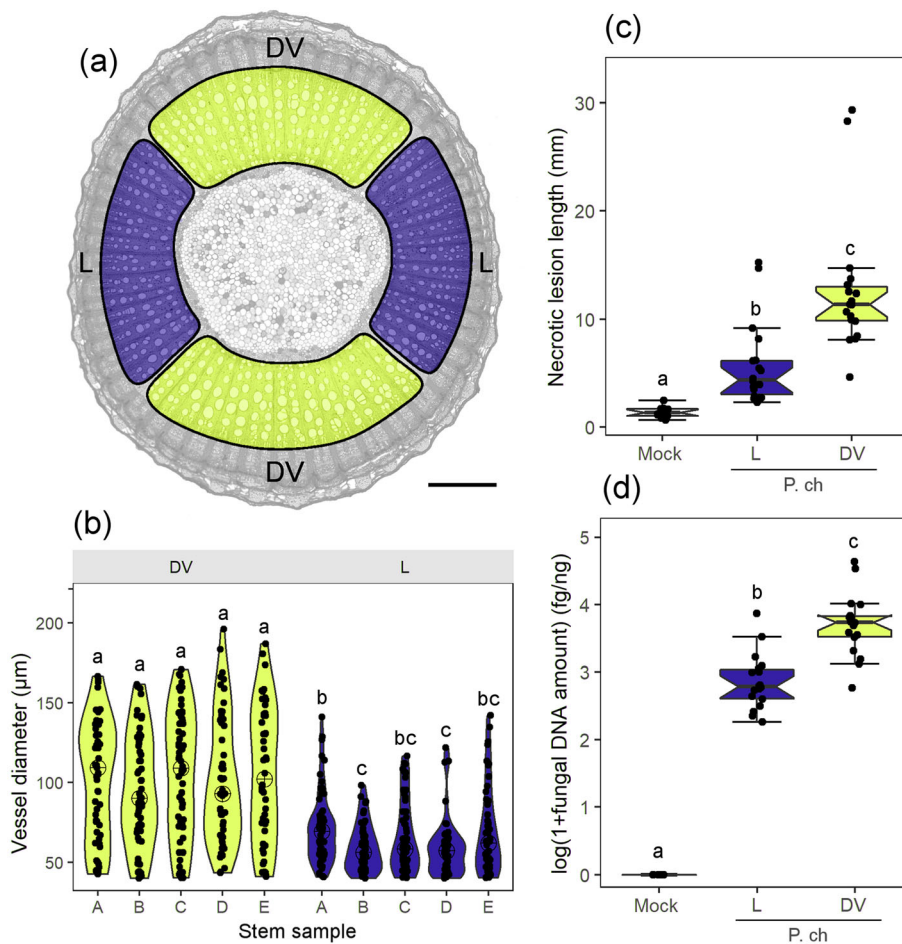


FIGURE 1 Effect of xylem vessel diameter (D_v) on grapevine susceptibility to *P. chlamydospora* with a single *V. vinifera* L. genotype. (a) Micrograph illustrating the difference in D_v distribution found across lateral (L) and dorso/ventral (DV) sector of 1-year-old stem of *V. vinifera* cv. Cabernet-Sauvignon (scale bar = 1,000 µm). (b) Distribution of D_v across L and DV sector of the stem. Different letters indicate significant differences at the .05 confidence level with a Dunn's test. (c,d) Level of infection of *V. vinifera* cv. Cabernet-Sauvignon measured 10 weeks after inoculation in lateral (L) or dorsal-ventral (DV) sector of the stem by (c) the necrotic lesion length (NLL) and (d) amounts of *P.ch* DNA (FDA) quantified by qPCR in xylem fragment remote from the inoculation wounds. Results presented are pooled data from two independent experimental replicates. Different letters indicate differences at the .05 confidence level with a Dunn's test (Mock control, $n = 10$; *P.ch* L and *P.ch* DV, $n = 18$). See Tables S1 and S2 for detailed statistical analyses

Finally, we tested the hypothesis that the efficiency of the compartmentalization process of a given vessel truly depends upon D_v . The parameterization of mechanistic models was undertaken to determine whether D_v effectively impacts the compartmentalization of the pathogen at the level of the xylem vessel.

2 | MATERIALS AND METHODS

2.1 | Testing the effect of vessel diameter distribution on host susceptibility within a single genotype

Resistance bioassays on a single cultivar were carried out on *V. vinifera* cv. Cabernet-Sauvignon (CS) selection #31. Structural differences in D_v distribution exist across DV (i.e., high amount of wide diameter vessels) and lateral sector (L; i.e., narrow vessels) of the stem in *V. vinifera* (Pouzoulet et al., 2014; Stevenson et al., 2004) (Figure 1a,b). Thus, inoculation in these different sectors of the stem was exploited to assess the effect of D_v on *P. chlamydospora* resistance within a single clonal population, and independently of other experimental factors. Certified cuttings were received from the FPS (Foundation Plant Services, University of California Davis, Davis, CA), propagated and grown as described by Pouzoulet et al. (2017). One-month-old

cuttings were wounded using a 3 mm diameter ethyl-alcohol sterilized drill to the pith 50 mm below the newly growth apical shoot. Plants were randomly selected and wounded either in the DV (90° from the axis of the buds) or in the lateral sector (0 or 180° from the axis of the buds). Inoculum consisted of a plug (3 mm in diameter) from a culture (Potato Dextrose Agar, Difco Laboratories, Franklin Lakes, NJ) of *P. chlamydospora* voucher isolate UCR-Pc4. Wounds were covered with parafilm. The experiment was replicated twice using different sets of cuttings at 1 month interval. Each experimental replicate consisted in a total of 23 plants, 9 plants being used for each of the two *P. chlamydospora* inoculation modalities (i.e., DV and L sectors) and 5 plants being inoculated with sterile PDA within the DV sector as Mock inoculated control.

After 10 weeks of incubation, stems were split open using a sterile razor blade in order to expose inner necrotic lesions. Pictures were taken using a stereomicroscope (M165C, Leica microsystems CMS GmbH, Wetzlar, Germany) and necrotic lesion lengths (NLL, Table 1, Figure S1) were measured using LAS v4.2 software (Leica microsystems CMS GmbH, Wetzlar, Germany). For the quantification of *P. chlamydospora* DNA in xylem fragments, stem samples from the wounded mock inoculated and *P. chlamydospora* inoculated plants were frozen and subjected to 48 hr of lyophilization using Labconco freezezone 2.5 L (Kansas City, MO). Samples were then cut longitudinally in the plane perpendicular to the inoculation wound in order to

recover only the half part of stems carrying the infection, as previously described by Pouzoulet et al. (2017). Then, a 15 mm long fragment was cut 15 mm above the top of the inoculation wound. Samples were ground with a mixer mill (MM 400, Retsch GmbH, Haan, Germany) and DNA was extracted as described previously (Pouzoulet, Mailhac, et al., 2013). The concentration of total DNA extracted was determined using a Qubit fluorometer and the Quant-it dsDNA high sensitivity reagent (Invitrogen, Carlsbad, CA) according to the manufacturer protocol. The qPCR reactions proceeded in a final volume of 25 μ l, and reaction mixtures contained 12.5 μ l of 2X SYBR Green Quantitect Master Mix (Qiagen, Venlo, Netherlands). Primers PchQF (5'-CTCTGGTGTGTAAGTTCAATCGACTC-3')/PchQR (5'-CCATTGTAGCTGTTCCAGATCAG-3') were used at a final concentration of 0.5 μ M. Two μ l of DNA template was used per reaction. Experiments were conducted with a CFX96 Real-Time PCR cycler using CFX manager software v3.1 (Bio-Rad, Irvine, CA). The cycling program consisted of (a) an initial denaturation step at 95°C for 15 min, (2) 40 cycles of 15 s at 95°C (for denaturation) followed by 45 s at 62°C (for both annealing and extension) and (3) an additional melting analysis of 40 min from 60 to 95°C. Preparation and use of standard solutions for the absolute quantification of *P. chlamydospora* isolate UCR-Pc4 DNA was done as previously described (Pouzoulet, Mailhac, et al., 2013). The average absolute amounts of *P. chlamydospora* DNA determined by qPCR in three independent technical replicates were standardized on the amounts of input DNA and used as the fungal DNA amounts (FDA, see Table 1) for further statistical analyses.

2.2 | Testing the effect of the density of wide diameter vessels on host susceptibility across genotypes

The hypothesis whereby vessel diameter impacts host susceptibility was tested through two different trials. In the first trial, referred to as the F2 trial, a subset of *Vitis* hybrid genotypes from a F2 progeny was used. This F2 progeny derives from a self-pollinated F1 hybrid *V. vinifera* cv. Cabernet-Sauvignon \times *Vitis riparia* cv. Gloire de Montpellier (CS \times RGM, Guillaumie et al., 2020). From this F2 progeny, 261 genotypes were previously characterized for xylem anatomy over 2 years, with highly contrasted phenotypes for D_v distribution (unpublished data). The entire progeny was maintained in a single greenhouse, grown in the same conditions and trained vertically on metallic wires with two lateral shoots. During the winter, dormant canes were collected and stored in a cold chamber until the next spring. Then, 34 genotypes were selected with (a) homogeneous cane diameter, and (b) the largest phenotypic range for morphological traits related to D_v distribution. Cuttings from one single cane per genotype were propagated as described above, and potted in 1 L plastic container in soil. Respective internode position from which cuttings were propagated was recorded. Plants were grown in a greenhouse following a complete random design. After a period of 1 month, they were inoculated with *P. chlamydospora* in the DV sector of the stem, using a solution of spores following Travadon, Gubler, Cadle-Davidson, Baumgartner, and Rolshausen (2013), with the sole difference being that

P. chlamydospora voucher isolate LR28 was used (Borie, Jacquot, Jamaux-Despréaux, Larignon, & Péros, 2002). For each genotype, between 4 and 6 plants were inoculated with *P. chlamydospora* (155 plants in total). A subset of 22 genotypes were used as control, 1–3 plants being inoculated with a sterile 100 mM PBS buffer (Mock inoculated pool of 37 plants). After 12 weeks of incubation, plants were analysed as described in the Section 2.1. Stems were split open using a sterile razor blade in order to expose inner necrosis. Pictures were taken using a reflex camera mounted on a stand, the samples being placed on a grid pattern. Sample names were blinded following a random design so that the experimenters could not know the identity of the sample analysed (i.e., genotype and treatment). Measurements of NLL were performed independently by two experimenters and the means were used for further analyses. For the absolute quantification of *P. chlamydospora* DNA by qPCR (i.e., FDA), 15 mm long wood samples were collected 10 mm above the top of the inoculation wound using a razor blade, and processed as described above. Healing at the wound was rated on a 4 scores scale, "0" being the total absent of bark ridge, "1" the presence of bark ridge at the margin of the wounds, "2" the presence of bark ridge at the margin and within the wound and "3" the presence of bark ridge that completely covered and filled the wound (see Figure S1). For each plant, a stem fragment was sampled about 50 mm above the inoculation wound and placed in 80% ethyl-alcohol for the analysis of xylem morphology. Fifty μ m slices covering the entire stem cross section were obtained using a GSL1 sledge microtome (Gärtner, Lucchinetti, & Schweingruber, 2014). Slices were stained using a 1% safranin O solution (96% ethyl-alcohol), rinsed twice in 100% ethyl-alcohol and transferred in xylene. Slices were then mounted between slide and coverslip in resin (Histolaque LMR, Labo-Moderne, Gennevilliers, France) and let dry for at least 24 hr. High-resolution micrographs (about 500 nm/pixel) were obtained at the Bordeaux Imaging Center, a member of the France Bio-Imaging national infrastructure (ANR-10-INBS-04) using a NANOZOOMER 2.0HT (Hamamatsu Photonics, Hamamatsu City, Japan) in brightfield mode. Measurements of xylem vessels were carried out on five consecutive fascicular portions located in the DV sector of the stem using ImageJ v1.52 (<https://imagej.nih.gov/ij/>) as described by Pouzoulet et al. (2017). The density of wide diameter vessels (DWV, see Table 1) was calculated as the count of vessels having a diameter superior to 100 μ m/mm² of cross-sectional area of xylem.

In the second trial, referred to as CG throughout this manuscript, a selection of 15 grapevine commercial genotypes (i.e., cultivars), *V. vinifera* L., were used: Sauvignon, Cabernet franc, Cabernet-Sauvignon, Grenache, Merlot, Sultanine, Chardonnay, Cinsaut, Clairette, Pinot noir, Saperavi, Syrah, Tempranillo, Tinta pinheira Ugni blanc. As opposed to the F2 trial, dormant canes from standing vines grown into the field were used to prepare vine cuttings. All mother-vines were grown in the same geographical location, at the INRAE Bordeaux-Nouvelle-Aquitaine Center (Vineyard Experimental Unit, Villenave-d'Ornon, France) and grafted on SO4 rootstocks. The assay consisted of 9–10 vines inoculated with *P. chlamydospora* (148 plants in total) and 5 control vines (Mock inoculated). Experiments and analyses were performed exactly as described for the F2 trial and at 2-week intervals.

2.3 | Statistical analysis

In all the experiments conducted in this study, the distribution (i.e., right skewed) of *NLL* (see Table 1) and *FDA* (see Table 1) justified the use of generalized linear modelling analyses with a gamma distribution so that the effect of various factors and covariates (i.e., specified in the tables of analyses outputs) can be tested. Post-analysis comparison of observed versus theoretical quantiles also supported this choice. Pairwise comparisons, when necessary, were performed using the Dunn's test and the FDR *p*-value correction method at a significance level of 5% (Benjamini & Hochberg, 1995).

The effect of *DWV* on *NLL* and *FDA* was assessed using a generalized linear mixed-effect modelling analysis with a gamma distribution, the trial (F2 or CG) being set as a random effect. The approach was performed using the whole dataset as well as different data binning approaches such as the mean values per genotypes, and the mean values per classes of *DWV*.

The effect of genotypes on healing scores was tested using the Kruskal–Wallis test. Correlations between healing scores and *NLL* or *FDA*, were tested using the Kendall rank correlation method. The effect of healing scores on *NLL*, or *FDA*, was also tested using generalized linear modelling analyses, considering healing scores as factors. All statistics were performed using R software v3.6 and the package lme4 (Bates, Mächler, Bolker, & Walker, 2014; R Core Team, 2019).

2.4 | Modelling the effect of vessel diameter on *NLL*

In order to determine which properties of the compartmentalization process were more likely affected by D_v , mechanistic models were developed and tested for their abilities to emulate *NLL* observed in susceptibility bioassays. We assumed that the *NLL* observed upon *P. chlamydospora* inoculation results from the colonization of individual vessels, which are independent from each other. Thus, we considered here for each cutting the colonization of each vessel individually (i.e., more than hundreds of vessels per cutting). The effect of D_v was tested on the (a) probability of escape once the fungus was compartmentalized ($P_{failure}$) and (b) distance the fungus spreads longitudinally in the vessels once escaping the compartmentalization process ($L_{failure}$), separately or in combination. Several events of escape, fungus spread and de novo effective compartmentalization occurring in series within a population of vessels of known D_v were emulated using a stochastic approach.

When considered, the effect of D_v on $P_{failure}$ was described using a logistic model as follow:

$$P_{failure} = P(D_v) = \frac{P_{max}}{1 + \exp(-\alpha \times D_v + \beta)} \quad (1)$$

where α and β are parameters of the model and P_{max} allow a maximum probability to be reached above a given value of D_v . When the

effect of D_v was not considered, $P_{failure}$ was assumed to be equal to 1 or set as a constant optimized in the model so that:

$$P_{failure} = cst, 0 < cst \leq 1 \quad (2)$$

When compartmentalization success was achieved, the length of the longitudinal spread of the fungus was considered null. The length of the longitudinal spread achieved in the case of an event of compartmentalization failure ($L_{failure}$) can be given by:

$$L_{failure} = \gamma \times a \quad (3)$$

where γ is a random variable uniformly distributed in the range of (0,1) and a is a coefficient allowing fungal longitudinal spread (i.e., and associated with predicted necrotic lesions) to differ in size. When the effect of D_v on the fungus spread was not considered, then a was set to 1. The effect of D_v on the fungus spread was described following an exponential relationship giving:

$$L_{failure} = \gamma \times a = \gamma \times \exp[\nu + (\mu \times D_v)] \quad (4)$$

where ν and μ are the intercept and slope of the exponential function, respectively. The final longitudinal colonization achieved in a given vessel (L_{tot}) is the sum of n independent consecutive events and can be given by:

$$L_{tot} = \sum_{i=1}^n (\epsilon(\delta_i - p_i) \times L_{failure} \times b) \quad (5)$$

where ϵ is the following step function:

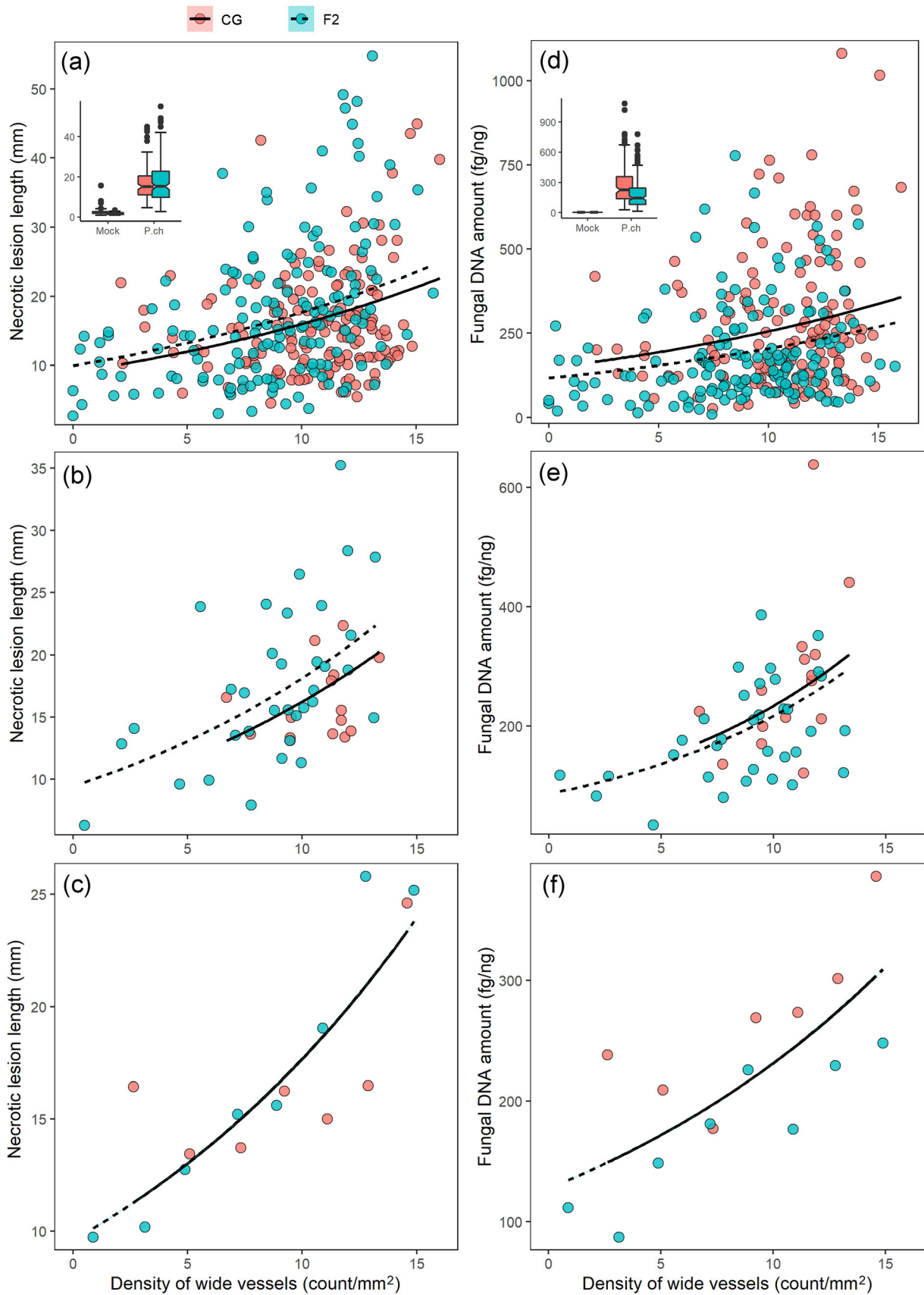
$$\epsilon(t) = \begin{cases} 0 & t \geq 0 \\ 1 & t < 0 \end{cases} \quad (6)$$

and where δ is a random variable uniformly distributed in the range of (0,1), and b a parameter allowing to scale the model with observed data. If we assume that the models are equally spaced time series of n events, then determining the probability of $P_{failure}$ can be considered as determining the probabilities of observing one or multiple events of compartmentalization failure after a given period of time. Thus, a change in n fundamentally results in a change of the time at which $P_{failure}$ is estimated, and consequently a change in $P_{failure}$ value itself. Because of this relationship between $P_{failure}$ and n , only $P_{failure}$ was allowed to be optimized, and n was arbitrary set to 10 events.

The length of the predicted necrosis (L_{pred}) for a given sample was considered to be the maximum longitudinal colonization predicted across all the vessels, and is given by:

$$L_{pred} = \max\{L_{totj}\}, j = \text{number of vessels} \quad (7)$$

A satisfactory mechanistic model should emulate the dispersion of observed *NLL* along the *DWV* gradient. For this reason, optimization of the parameters of the models was achieved by minimizing the root mean square errors (RMSE) of both the moving average and the

**FIGURE 2** Legend on next page.

95% interval boundaries of the predicted versus observed *NLL* data using a genetic algorithm. The observed moving averages and 95% confidence boundaries were plotted against the values predicted by the models, and the slopes and the intercepts of the regression were adopted to evaluate the goodness of fit. Due to the stochastic properties of the model, each simulation of a given model results in a unique outcome. For these reasons, comparison across models were performed using mean values (RMSE and observed vs. predicted regression line parameters) from 500 simulations of each model. Modelling was performed on R software v3.6 using the “GA” package (R Core Team, 2019; Scrucca, 2013).

3 | RESULTS

3.1 | Testing the effect of vessel diameter distribution on host susceptibility within a single genotype

The effect of D_v on *P. chlamydospora* susceptibility was first tested on a single genotype (i.e., *V. vinifera* cv. CS) by exploiting structural differences existing across DV (i.e., high *DWV*) and L sectors (i.e., low *DWV*) of the stem. From five 1-year-old shoots of five grapevine cv. CS representative of the material used in these bioassays, there is a major and significant effect of the anatomical location (i.e., L vs. DV) on D_v distribution ($p < .001$) (Figure 1a,b, Table S1). A small but significant effect ($p = .02$) of the stem sample was also found.

From *P. chlamydospora* inoculation bioassays, a significant effect of the inoculation ($p < .001$) and the anatomical location of the inoculation wound ($p < .001$) on *NLL* developed after 10 weeks was observed (Figure 1c, Table S2). There were no effects of biological replicates ($p = 0.36$). The Mock inoculated plants developed the shortest *NLL*. The longest *NLL* were observed in plants inoculated in the DV sector of the stem, where a high *DWV* is present. Plants inoculated in the L sector of the stem, where the *DWV* is low, developed *NLL* significantly longer than the Mock control but significantly shorter than the plant inoculated in the DV sector of the stem (Figure 1c).

FDA measured within xylem fragments remote from the inoculation wounds depicted similar results (Figure 1d, Table S2). Because *P. chlamydospora* DNA was not detected from Mock inoculated plant samples, they were not included in the analysis. Analysis of variance showed a significant effect of the inoculation location ($p < .001$) and no effect of biological replicates on *FDA* ($p = .08$). Significantly higher *FDA* was quantified within DV inoculated plants compared to L inoculated plants, supporting observations from *NLL* (Figure 1d).

3.2 | Testing the effect of the density of wide diameter vessels on host susceptibility across genotypes

From both F2 and CG trials, there was a highly significant effect ($p < .001$) of the genotypes on the *DWV* (Table S3, Table S4, Figure S2, Figure S3). For the F2 trial, a small but significant ($p = .03$) effect of the internode position from which the cuttings were produced was also observed, reflecting the fact that the average D_v and by consequence *DWV* decreased along sampled canes (Table S3). Highly significant effects of *P. chlamydospora* inoculation (Mock vs. *P. chlamydospora* inoculation, $p < .001$) and genotypes ($p < .001$) on *NLL* were also present for both trials (Table S3, Table S4, Figure S4, Figure S5, see also the inset in Figure 2a). Fungal DNA was never detected in Mock inoculated (control) plants while it was consistently detected in all *P. chlamydospora* inoculated plants (inset in Figure 2d). Thus, control plants were not considered for further statistical analysis of *FDA*. For *P. chlamydospora* inoculated plants, genotypes had a significant effect on *FDA* in both F2 and CG trials ($p < .001$) (Table S3, Table S4, Figure S6, Figure S7).

Our data showed that there was a significant relationship between the *DWV* and *NLL*, and *DWV* and *FDA* ($p < .001$; Figure 2a,d, Table S5). The relation between *DWV* and *NLL*, and *DWV* and *FDA*, was conserved when visualizing those relationships using both averaged values per genotype (Figure 2b,e, Table S5), and binned data from different *DWV* classes (Figure 2c,f, Table S5).

Comparison of *NLL* and *FDA* on the whole dataset revealed that there was a low but significant correlation between these two variables (pseudo- $R^2 = .19$, $p < .001$) (Figure 3a, Table S6). The relationship was slightly improved using mean values per genotypes (pseudo- $R^2 = .22$; Figure 3b). The relationship was however drastically improved by using bin values per wide vessel diameter vessel classes (pseudo- $R^2 = .79$; Figure 3c). There was also a significant effect of the trials, indicating the relationship between *NLL* and *FDA* likely depended on plant material used in these experiments (Figure 3). Overall, a given *FDA* was associated with longer *NLL* in the CG trial (i.e., pure *V. vinifera* species) compared to the F2 trials (*V. vinifera* × *V. riparia* hybrids).

We used the healing score as a proxy for a genotype's ability to mitigate the effect of infection and related this to *NLL* and *FDA*. In both CG and F2 trials, all Mock treated plants exhibited extensive amounts of healing tissue (i.e., bark ridge) covering the inoculation wounds (Figure S1, Figure 4a). However, genotype's ability to heal upon *P. chlamydospora* infection was highly variable, especially within the F2 trial (Figures 4a, Figure S8, Figure S9). Within the F2

FIGURE 2 Effect of wide diameter vessel density (*DWV*) on necrotic lesion length (*NLL*) and *P. chlamydospora* DNA amount (*FDA*) in two different trials. Plants corresponding to the grapevine commercial cultivar trial (CG) are represented in red and full lines, and F2 CS × RGM progeny trial (F2) are represented in green and dashed lines. The relationships between the *NLL* (a,c) or *FDA* (d-f) versus the *DWV* are represented using different binning methods: (a,d) whole data set; (b,e) mean values per genotypes; (c,f) mean values per classes of wide diameter vessels (*DWV* classes steps = 2 counts per mm²). (a and d insets) The comparison of Mock versus *P. chlamydospora* inoculated plants is provided as insets in the boxplot in the top-left corner. The regression lines correspond to the predictions given by the generalized linear mixed modelling analysis (CG trials: full line; F2 trial: dashed line; see Table S5)

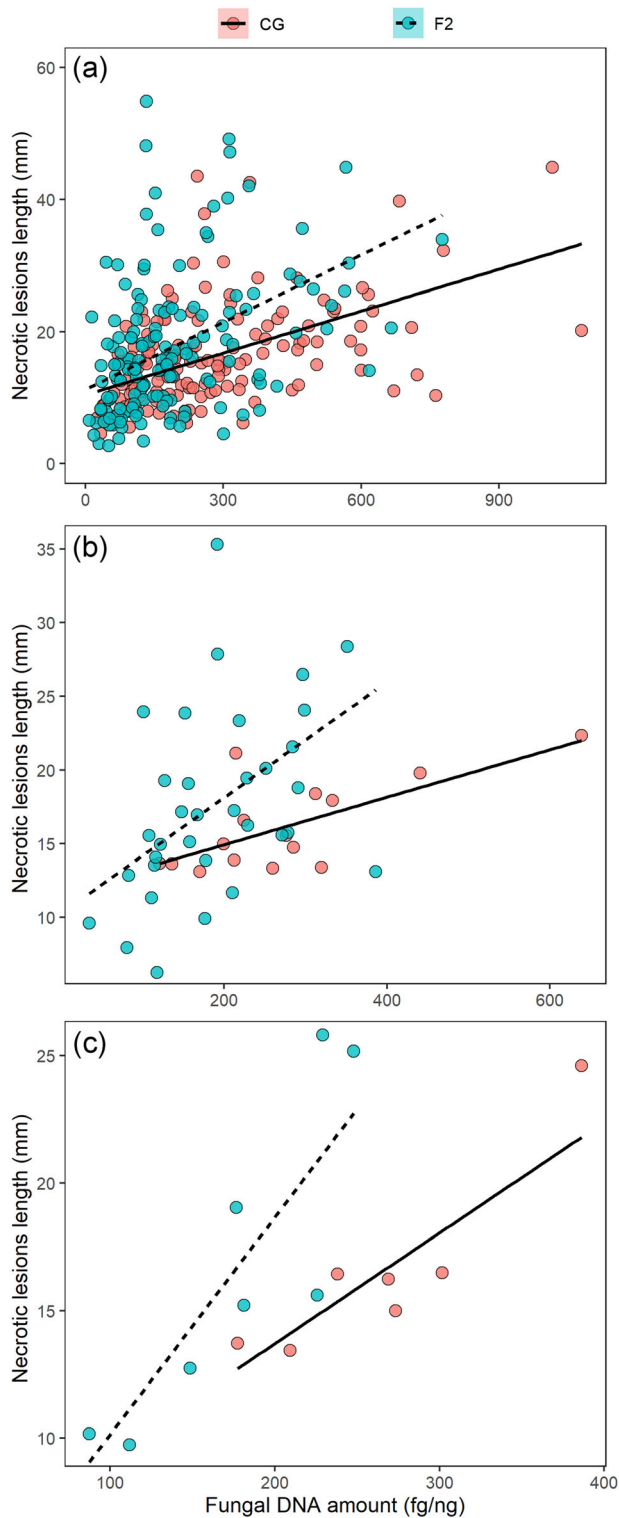


FIGURE 3 Relationship between necrotic lesion length (NLL) and *P. chlamydospora* DNA amount (FDA) from the grapevine commercial cultivar trial (CG; in red and full lines) and F2 CS × RGM progeny trials (F2; green and dashed lines). Different data binning methods are presented such as in Figure 2: (a) whole data set; (b) mean values per cultivars and genotypes and (c) mean values per classes of wide diameter vessels (DWV classes steps = 2 counts per mm²). Regression lines were obtained from generalized linear modelling analyses (see Table S6)

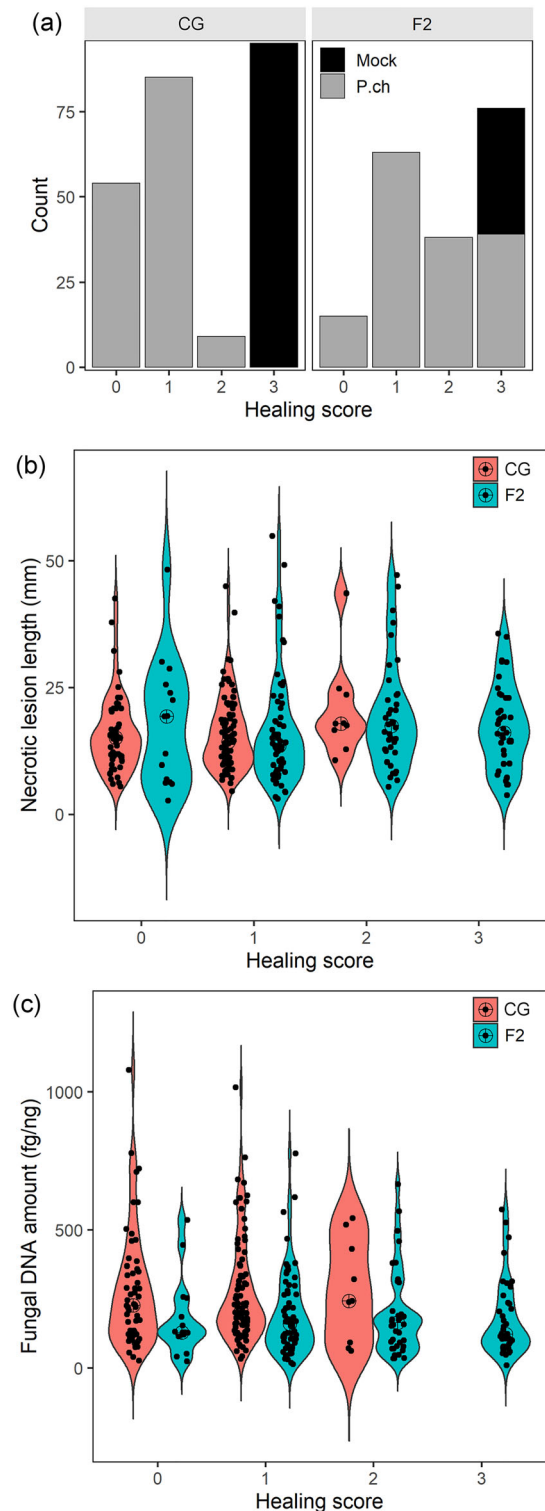


FIGURE 4 Absence of relationship between the healing phenotype observed upon inoculation and the level of susceptibility to *P. chlamydospora* measured through necrotic lesion length (NLL) and fungal DNA amount (FDA) in commercial grapevine genotypes (CG) and F2 CS × RGM progeny (F2). (a) Bar charts showing the absolute counts for the different healing scores observed in the grapevine commercial cultivars and F2 progeny bioassays upon Mock and *P. chlamydospora* inoculation. (b,d) Distribution of NLL (b) and FDA (c) observed across healing scores in the two trials. See Table S7 and the main text for detailed statistical analysis. See Figure S1 for detailed explanation about the healing score used

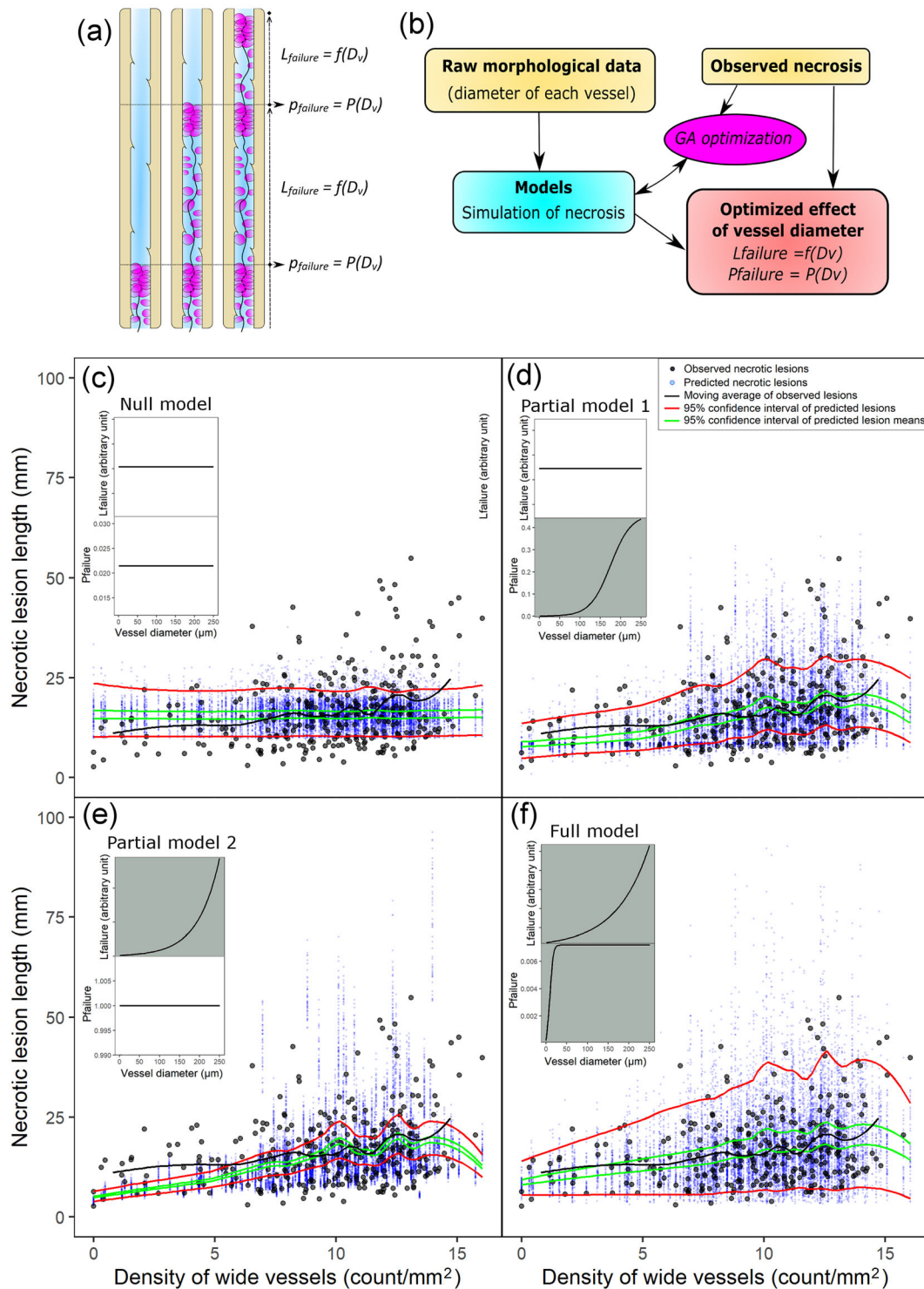


FIGURE 5 Evaluation of the effect of xylem vessel diameter (D_v) on compartmentalization processes by a modelling approach. (a) Schematic representation of the hypotheses tested in the models for the effect of D_v on *P. chlamydospora* compartmentalization. The vessel lumen is schematized in blue, the tyloses in purple and the fungal hyphae by the winding black line running through the vessel lumen. (b) Diagram of the global approach used to evaluate the effect of D_v on compartmentalization processes. (c–f) Plots displaying prediction abilities of the models tested. The respective optimized effects of D_v on $L_{failure}$ and $P_{failure}$ are presented in inlays at the top right corner of each plot. Note that differences between models lie on the differential allowance given for the optimization of $L_{failure}$ and $P_{failure}$ as a function of D_v (top-left corner insets filled in grey when allowed). Predicted necrotic lesion lengths (NLL, blue dots) and respective predicted 95% intervals based on 50 simulations of each model are presented here for a purpose of clarity. Note that 500 simulations were used to optimized models parameters. See Figure S10 and Table S8 for further information about model parameters and validation statistics

CS \times RGM progeny, average healing scores ranged from 0.3 (i.e., an absence of the healing process in almost all replicates) to 3 (i.e., all replicates healed similarly to the Mock control) (Figure S8). Within the CG trial, a lower ability to heal upon infection was noticed with the average healing score ranging from 0 to 1.3 (Figure S9). Significant differences occurred across genotypes for this trait in both the CG and F2 trials (Kruskal–Wallis test, $p < .001$). There was no significant effect of healing score neither on *NLL* nor on *FDA* (Figure 4b,c, Table S7).

3.3 | Modelling the effect of anatomical measurement on *NLL*

In silico modelling confirmed that necrotic lesions observed in susceptibility trials can be emulated when the effect of D_v on the compartmentalization processes is implemented at the level of each individual vessel (Figure 5, Figure S10). This approach allowed us to test diverse biological scenarios and to assess the effect of D_v on two compartmentalization features (i.e., $L_{failure}$, $P_{failure}$) (Figure 5a,b).

We first tested whether data observed in our susceptibility trials could be reproduced by a “null” model, whereby D_v had no effect on $L_{failure}$ or $P_{failure}$ (Figure 5c). The best fit obtained using this “null” model resulted in the lack of *DWV* effect on the predicted *NLL* and a poor prediction of their upper and lower 95% confidence intervals, as seen through the deviation of the observed vs. predicted regression curve from the 1:1 line (Figure S10a, Table S8). Allowing D_v to impact only $L_{failure}$ or $P_{failure}$ resulted in an improvement of goodness of fit of models (i.e., referred as model “partial 1” and “partial 2”) as seen by a better predictions of both mean *NLL* and data dispersion (Figure 5d,e, Figure S10) compared to the “null” model. The regression lines of the observed vs. predicted values also significantly deviated from the 1:1, indicating that these two models were not able to truly emulate the overall dispersion of data (Figure S10b,c, Table S8). Allowing the optimization of both $L_{failure}$ and $P_{failure}$ (i.e., referred as “full model”) resulted in the most satisfactory model (Figure 5f). Although a higher average RMSE value was obtained for this “full” model compared to the models “partial 1” and “partial 2”, the observed vs. prediction regression lines from 500 simulations were consistently fitting closely to the 1:1 line (Figure S10d, Table S8). Across simulations, the lowest RMSE value was also obtained by the “full” model, supporting its better ability to emulate the dataset from our susceptibility trials (Table S8). The solutions found in this “full” model for the effect of D_v on $L_{failure}$ and $P_{failure}$ attributed the main effect of D_v on $L_{failure}$ (Figure 5f insets). In contrast, the effect of D_v attributed to $P_{failure}$ can be considered null, $P_{failure}$ reaching a plateau of fairly low probability (i.e., $P_{failure} = .007$) at a D_v value of about 30 μm (Figure 5f insets).

4 | DISCUSSION

This study provides new evidence about the role of plant vascular structure in host susceptibility to pathogen attack. We validated this concept using a model pathosystem between grapevine and the

vascular pathogen *P. chlamydospora*. Our data supported the hypothesis that the heterogeneity in D_v distribution across host genotypes, and within a single host genotype, impacts host susceptibility. Finally, we demonstrated in silico that change in susceptibility observed in our experimental trials can be explained by modification in the compartmentalization efficiency of the pathogen, which depends on the D_v of individual xylem vessels.

One can assume that if D_v has an impact on the efficiency of the compartmentalization process, and thus pathogen movement, then a change in D_v distribution necessarily results in an effective change in host susceptibility to the pathogen. This assumption was validated, whereby cuttings of a single genotype inoculated within sector of the stem harbouring low D_v (lateral sector) were significantly less susceptible (i.e., smaller *NLL* and lower *FDA*) than plants inoculated within sector harbouring higher D_v values (*DV* sector). Previous works on Dutch elm disease suggested that the modification of D_v distribution induced by differential irrigation regime corresponds to a change in host susceptibility to the disease it causes, likely due to its impact on pathogen movement (Solla & Gil, 2002b). It can be hypothesized that a similar relationship also exists in the case of the esca disease of grapevine, disease incidence being positively correlated to rainfall and host vigour (Calzarano, Osh, Baranek, & Marco, 2018; Guérin-Dubrana et al., 2013; Pouzoulet et al., 2014). Variations of host susceptibility could stem from other physiological trade-offs between growth and constitutive defence, making it difficult to assess the contribution of xylem morphology on host susceptibility (Hahn & Maron, 2016; Porth, White, Jaquish, & Ritland, 2018). Because we exploited the morphological heterogeneity found within the grapevine stem, our experimental design was unbiased by other experimental factors such as genetic background and abiotic treatments.

To date, no *Vitis* genotypes were found to be fully immune (i.e., non-host interaction) to *P. chlamydospora* (Bertsch et al., 2013; Eskalen, Gubler, & Khan, 2001; Martínez-Diz et al., 2019; Travadon et al., 2013). Differences in pathogen susceptibility has been reported within the literature across *V. vinifera* genotypes and *Vitis* hybrid rootstocks (Eskalen et al., 2001; Martínez-Diz et al., 2019; Pouzoulet et al., 2017), suggesting that complex and multigenic types of resistance or tolerance are likely involved (Michelmoré, Christopoulou, & Caldwell, 2013; Snieszko & Koch, 2017). Our results confirmed that xylem structure is a driver of grapevine resistance to the *P. chlamydospora* infection. In addition to the measurement of *NLL* usually performed in such susceptibility studies, fungal infection level was also assessed by measuring *FDA* in host tissues using a sensitive molecular approach. The *NLL* is a measure of symptom development, and thus of the consequence of the pathogen colonization in host tissues while the *FDA* is a measure of the overall pathogen load within these tissues. Although they both result from the colonization of the host by the pathogen, they might reflect different aspects of the infection process, and it is understandable that they do not correlate strongly in practice on a plant-to-plant basis. Nonetheless, these two observations support the same biological conclusion about the impact of *DWV* on host resistance to the pathogen.

Our results support that the compartmentalization of vascular pathogens, and thus their colonization of the plant vascular system, is not a continuous process. Beckman and Roberts (1995) proposed that

the successful, systemic colonization of a plant host by vascular wilt pathogens such as *Verticillium* and *Fusarium* spp. involves a series of pathogen entrapment and compartmentalization, followed by compartmentalization escape and de novo pathogen spread. The mechanistic models we tested depict such a scenario, whereby the diameter of a vessel potentially affects (a) the probability of pathogen escape from the compartmentalization process ($P_{failure}$) and (b) the extent of pathogen spread in case of compartmentalization failure ($L_{failure}$). Based on data from our susceptibility trials, we can conclude that differences in susceptibility attributed to xylem morphology mostly translate into an increased likelihood of cuttings with large *NLL* and *FDA* with increasing *DWV*. Nonetheless, cuttings with short *NLL* and low *FDA* were also consistently observed along the *DWV* gradient. These observations are consistent with those previously reported, where a larger variability in *NLL* is observed in susceptible compared to more resistant genotypes (Martínez-Diz et al., 2019; Pouzoulet et al., 2017; Travadon et al., 2013). These experimental observations support that decreased host resistance does not systematically result in higher infection severity, but rather with an increased risk of severe infection to occur. We can conclude that determining with confidence the true level of resistance of a given genotype relative to others through inoculation bioassays is virtually impossible unless highly standardized plant material and high number of replicates are used, making such screening task particularly challenging in practice. D_v distribution is a plastic trait that has been reported to vary to a large extent depending on environmental conditions, shoot orientation and position along the plant axis, and plant size and age (Lovisolo & Schubert, 1998; Martín et al., 2013; Rosell, Olson, & Anfodillo, 2017; Schubert, Lovisolo, & Peterlunger, 1999). It would be interesting to determine if the plant material shows the same trends for xylem characteristics in response to these factors, and to examine in these contexts whether differences in xylem characteristics between cultivars are consistently related to *P. chlamydospora* resistance.

In vascular wilt pathosystems, the colonization of the host is mostly achieved by spores or propagules that are passively carried through the plant via transpiration (Beckman & Roberts, 1995; Yadeta & Thomma, 2013). Once a vessel becomes infected, spores would travel only so far before being physically entrapped by plates at the vessel ends. Since the vessel diameter represents a good proxy for its length in grapevine (Liu, Pan, & Tyree, 2018), the occurrence of end-walls along the colonization path could contribute to the variation of resistance observed across vessels having different D_v . The inoculation wound performed in this present study resulted in extensive damage of vessels and subsequent disruption of the water column at the vicinity of the wound. As a consequence, the effect of D_v should be interpreted here in a context of active colonization of vessels by the fungal hyphae, rather than passive dissemination of spores carried by the sap flow. The necrosis length found in our experiments suggested that the fungus only progressed a few centimetres from the inoculation wound, falling well below the expected average length of open vessels in grapevine stem (Chatelet et al., 2011; Liu et al., 2018). Although the effect of vessel length on pathogen movement should be further examined, its role is questionable in our experimental conditions.

The most satisfactory model depicted a scenario where D_v has an impact on the spread of the pathogen once it manages to escape, but no effect on the probability that the pathogen will escape. *P. chlamydospora* was found to spread by means of hyphae in the narrow spaces formed at the intersection of the tylosis because this pectin-rich substrate likely provides a carbon source for the pathogen (Marchi, Roberti, D'Ovidio, Mugnai, & Surico, 2001; Morales-Cruz et al., 2015; Pouzoulet et al., 2017). In addition, the increase in the number of tylosis observed with increasing D_v could provide a higher number of alternative routes for the pathogen to colonize occluded vessels (Pouzoulet et al., 2017). It was also hypothesized that the effect of D_v on the kinetic of vessel occlusion could have detrimental effects of vessel ability to limit the pathogen movement (Pouzoulet et al., 2019). Our model does not support that D_v impacts the likelihood of compartmentalization failure. It nonetheless suggests that the probability of observing compartmentalization escape is extremely low which could be interpreted as an effective ability of the host to eliminate the pathogen once it is compartmentalized, as described in other vascular pathosystems (Fradin & Thomma, 2006; Yadeta & Thomma, 2013). In line with this hypothesis, Valtaud, Larignon, Roblin, and Fleurat-Lessard (2009) reported the presence of damaged hyphae in the xylem of *P. chlamydospora* experimentally infected cuttings. The redistribution of this low probability over a high number of vessels explains the observed variability of infection severity.

We observed a large variability in the ability of genotypes from the F2 interspecific cross to heal and restore vascular cambium integrity upon infection. The capacity of perennial plants to protect and maintain vascular cambium integrity upon biotic aggression is pivotal to ensure host longevity because it retains their ability to regenerate functional secondary vascular tissues (Pearce, 1996). *P. chlamydospora* is known to secrete a set of phytotoxins having detrimental effects on host metabolism (Bruno, Sparapano, & Graniti, 2007; Luini, Fleurat-Lessard, Rousseau, Roblin, & Berjeaud, 2010; Pierron et al., 2016). While the ability of a given genotype to limit the fungus spread would match with the definition of resistance as it affects the size of pathogen population within the host, the ability to heal upon infection would match with the definition of tolerance as it relies on the capacity of the host to maintain proper physiological functions upon infection, such as the cellular proliferation and growth required in bark ridge development (Pouzoulet, Jacques, Besson, Dayde, & Mailhac, 2013; Shigo, 1984). It is worth noticing these two traits were not related to each other, supporting that the efficacy of pathogen compartmentalization was mainly a function of morphological features. This finding raises questions about the potential weight of these different traits (i.e., resistance vs. tolerance) on the overall host susceptibility as seen in the field. The *NLL* has been widely used as a marker of genotype susceptibility to vascular pathogen (Cruickshank, Bleiker, Sturrock, Becker, & Leal, 2018; Eskalen et al., 2001; Travadon et al., 2013). On the other hand, bioassays performed on detached leaves, callus and in vitro plantlets, also stressed that physiological processes, such as the induction of defence, were differentially affected across genotypes while they are exposed to the wood pathogens or to the toxins they secreted (Cardot et al., 2019; Lambert

et al., 2013; Stempien et al., 2018). Recent advances on esca disease aetiology strongly suggested that symptoms are indeed triggered in a remote fashion, the causal agents being absent from symptomatic organs (stems of year and leaves) while present into the trunk (Bortolami et al., 2019). Lessons from other vascular pathosystems showed that the compartmentalization of the pathogen represents a first line of defence, its efficacy having a significant contribution to the overall disease outcome (Beckman & Roberts, 1995; Fradin & Thomma, 2006). Mechanisms of tolerance can therefore operate independently of those of resistance to mitigate the effects of infection on host physiology, and promote its performance and longevity (Cruickshank et al., 2018; Fradin & Thomma, 2006; Rusli, Idris, & Cooper, 2015). In contrast to genotypes from the F2 progeny, all pure *V. vinifera* genotypes tested in this study presented a poor healing ability upon *P. chlamydospora* infection. We can hypothesize that this trait inherited from *V. riparia* rather than *V. vinifera*. Infection by *P. chlamydospora* has been associated with leaf scotch and wilt symptoms known as Petri disease and esca disease (Larignon & Dubos, 1997; Mugnai, Graniti, & Surico, 1999). The first case of esca disease foliar symptoms was reported in 1890 in the state of New York, while esca disease was absent in Europe at that time (Surico, 2009). Most if not all diseases encountered today in commercial vineyards were introduced from Northern-America during the second half of the 19th century (Travadon et al., 2012). For more than a century now, native *Vitis* spp. from Northern-America such as *V. riparia* have been extensively used as a source of genetic resistance towards pests and diseases (Barba et al., 2018; Merdinoglu, Schneider, Prado, Wiedemann-Merdinoglu, & Mestre, 2018; Riaz, Krivanek, Xu, & Walker, 2006; Rubio et al., 2020; Smith et al., 2018). One can hypothesize that *V. riparia* coevolved with *P. chlamydospora* and developed tolerance mechanisms towards this pathogen. Further research is now required in order to clarify the respective impact of mechanisms of resistance and tolerance described here on the overall susceptibility of grapevine hosts to the diseases, as seen in the field.

5 | CONCLUSIONS

Despite tremendous progress made in the past decades about the molecular nature of plant–pathogen interactions, particularly regarding our understanding of host resistance to microbial aggression, other basic physiological mechanisms, such as the impact of host structural traits on its response to infection have been overlooked. We provide evidence that xylem vessel diameter has a significant impact on compartmentalization efficiency and thus host defence capability in a major perennial crop, grapevine. Because of the basic nature of physiological mechanisms that are likely involved, we believe that this concept could be relevant in a wider variety of plant vascular pathogens and hosts.

ACKNOWLEDGMENTS

The authors thank Jean-Pierre Péros (Institut Agro INRAE, UMR AGAP) for the donation of the *P. chlamydospora* LR28 voucher isolate.

The authors would like to thank the Foundation Plant Service (University of California Davis) and the INRAE Bordeaux-Nouvelle-Aquitaine Vineyard Experimental Unit for donating some plant material used in this research. The authors also thank David Carter (Center of Plant Cell Biology, University of California Riverside) and Sébastien Marais (Université de Bordeaux/CNRS, Bordeaux Bio-Imaging Center) for their useful assistance and advice on microscopy. The authors would also like to thank the technical staff of UMR EGFV and UMR SAVE and in particular Sébastien Gambier, Jean-Pierre Petit and Jean-Pascal Tandonnet for their helpful assistance in the preparation of plant material. This research was funded by the French Ministry of Agriculture, Agrifood, and Forestry (FranceAgriMer and CNIV) within the PHYSIOPATH project (program Plan National Dépérissement du Vignoble, #22001150-1506 awarded to C. E. L. D.), the European Union Commission (Marie Skłodowska-Curie Action, Agreskill+ Grant #1357 awarded to J. P.), the Région Nouvelle-Aquitaine (Grant #2017-1R20209 awarded to N. O.) and the U.S. Department of Agriculture (National Institute of Food and Agriculture, Specialty Crop Research Initiative, grant #2012-51181-19954). This research received financial support from the INRAE department “Biologie et Amélioration des Plantes.”

CONFLICT OF INTEREST

The authors declare that they have no conflict of interest.

ORCID

Jérôme Pouzoulet  <https://orcid.org/0000-0002-9890-7377>

Chloé E. L. Delmas  <https://orcid.org/0000-0003-3568-605X>

REFERENCES

- Ácímović, S. G., Martin, D. K. H., Turcotte, R. M., Meredith, C. L., & Munck, I. A. (2019). Choosing an adequate pesticide delivery system for managing pathogens with difficult biologies: Case studies on *Diplodia corticola*, *Venturia inaequalis* and *Erwinia amylovora*. *Plant Diseases-Current Threats and Management Trends*. <https://doi.org/10.5772/intechopen.87956>
- Barba, P., Lillis, J., Luce, R. S., Travadon, R., Osier, M., Baumgartner, K., ... Cadle-Davidson, L. (2018). Two dominant loci determine resistance to Phomopsis cane lesions in F1 families of hybrid grapevines. *Theoretical and Applied Genetics*, 131(5), 1173–1189. <https://doi.org/10.1007/s00122-018-3070-1>
- Bates, D., Mächler, M., Bolker, B., & Walker, S. (2014). Fitting linear mixed-effects models using lme4. *ArXiv*, 51. <http://arxiv.org/abs/1406.5823>
- Beckman, C. H., & Roberts, E. M. (1995). *On the nature and genetic basis for resistance and tolerance to fungal wilt diseases of plants*, 21(35–77). Cambridge, Massachusetts, USA: Academic Press.
- Beckman, C. H., Vandermolén, G. E., Mueller, W. C., & Mace, M. E. (1976). Vascular structure and distribution of vascular pathogens in cotton. *Physiological Plant Pathology*, 9(1), 87–94. [https://doi.org/10.1016/0048-4059\(76\)90078-3](https://doi.org/10.1016/0048-4059(76)90078-3)
- Benjamini, Y., & Hochberg, Y. (1995). Controlling the false discovery rate: A practical and powerful approach to multiple testing. *Journal of the Royal Statistical Society: Series B (Methodological)*, 57(1), 289–300. <https://doi.org/10.1111/j.2517-6161.1995.tb02031.x>
- Bertsch, C., Ramírez-Suero, M., Magnin-Robert, M., Larignon, P., Chong, J., Abou-Mansour, E., ... Fontaine, F. (2013). Grapevine trunk diseases: Complex and still poorly understood. *Plant Pathology*, 62(2), 243–265. <https://doi.org/10.1111/j.1365-3059.2012.02674.x>

- Borie, B., Jacquot, L., Jamaux-Despréaux, I., Larignon, P., & Péros, J.-P. (2002). Genetic diversity in populations of the fungi *Phaeoconiella chlamydospora* and *Phaeoacremonium aleophilum* on grapevine in France. *Plant Pathology*, 51(1), 85–96. <https://doi.org/10.1046/j.0032-0862.2001.658.x>
- Bortolami, G., Gambetta, G. A., Delzon, S., Lamarque, L. J., Pouzoulet, J., Badel, E., ... Delmas, C. E. L. (2019). Exploring the hydraulic failure hypothesis of esca leaf symptom formation. *Plant Physiology*, 181(3), 1163–1174. <https://doi.org/10.1104/pp.19.00591>
- Bouda, M., Windt, C. W., McElrone, A. J., & Brodersen, C. R. (2019). In vivo pressure gradient heterogeneity increases flow contribution of small diameter vessels in grapevine. *Nature Communications*, 10(1), 1–10. <https://doi.org/10.1038/s41467-019-13673-6>
- Brodersen, C. R., Choat, B., Chatelet, D. S., Shackel, K. A., Matthews, M. A., & McElrone, A. J. (2013). Xylem vessel relays contribute to radial connectivity in grapevine stems (*Vitis vinifera* and *V. arizonica*; Vitaceae). *American Journal of Botany*, 100(2), 314–321. <https://doi.org/10.3732/ajb.1100606>
- Bruno, G., Sparapano, L., & Graniti, A. (2007). Effects of three esca-associated fungi on *Vitis vinifera* L.: IV. Diffusion through the xylem of metabolites produced by two tracheiphilous fungi in the woody tissue of grapevine leads to esca-like symptoms on leaves and berries. *Physiological and Molecular Plant Pathology*, 71(1), 106–124. <https://doi.org/10.1016/j.pmp.2007.12.004>
- Calzarano, F., Osh, F., Baranek, M., & Marco, S. D. (2018). Rainfall and temperature influence expression of foliar symptoms of grapevine leaf stripe disease (esca complex) in vineyards. *Phytopathologia Mediterranea*, 57(3), 488–506. https://doi.org/10.14601/Phytopathol_Mediterr-23787
- Cardot, C., Mappa, G., la Camera, S., Gaillard, C., Vriet, C., Lecomte, P., ... Coutos-Thévenot, P. (2019). Comparison of the molecular responses of tolerant, susceptible and highly susceptible grapevine cultivars during interaction with the pathogenic fungus *Eutypa lata*. *Frontiers in Plant Science*, 10. <https://doi.org/10.3389/fpls.2019.00991>
- Chatelet, D. S., Matthews, M. A., & Rost, T. L. (2006). Xylem structure and connectivity in grapevine (*Vitis vinifera*) shoots provides a passive mechanism for the spread of bacteria in grape plants. *Annals of Botany*, 98(3), 483–494. <https://doi.org/10.1093/aob/mcl124>
- Chatelet, D. S., Wistrom, C. M., Purcell, A. H., Rost, T. L., & Matthews, M. A. (2011). Xylem structure of four grape varieties and 12 alternative hosts to the xylem-limited bacterium *Xylella fastidiosa*. *Annals of Botany*, 108(1), 73–85. <https://doi.org/10.1093/aob/mcr106>
- Cruikshank, M. G., Bleiker, K. P., Sturrock, R. N., Becker, E., & Leal, I. (2018). Resistance and tolerance of Douglas-fir seedlings to artificial inoculation with the fungus *Ophiostoma pseudotsugae*. *Forest Pathology*, 48(5), e12437. <https://doi.org/10.1111/efp.12437>
- Deyett, E., Pouzoulet, J., Yang, J.-I., Ashworth, V. E., Castro, C., Roper, M. C., & Rolshausen, P. E. (2019). Assessment of Pierce's disease susceptibility in *Vitis vinifera* cultivars with different pedigrees. *Plant Pathology*, 68(6), 1079–1087. <https://doi.org/10.1111/ppa.13027>
- Eskalen, A., Gubler, W. D., & Khan, A. (2001). Rootstock susceptibility to *Phaeoconiella chlamydospora* and *Phaeoacremonium* spp. *Phytopathologia Mediterranea*, 40, S433–S438.
- Fradin, E. F., & Thomma, B. P. H. J. (2006). Physiology and molecular aspects of Verticillium wilt diseases caused by *V. dahliae* and *V. albo-atrum*. *Molecular Plant Pathology*, 7(2), 71–86. <https://doi.org/10.1111/j.1364-3703.2006.00323.x>
- Gärtner, H., Lucchinetti, S., & Schweingruber, F. H. (2014). New perspectives for wood anatomical analysis in dendrosciences: The GSL1-microtome. *Dendrochronologia*, 32(1), 47–51. <https://doi.org/10.1016/j.dendro.2013.07.002>
- Gramaje, D., Baumgartner, K., Halleen, F., Mostert, L., Sosnowski, M. R., Úrbez-Torres, J. R., & Armengol, J. (2016). Fungal trunk diseases: A problem beyond grapevines? *Plant Pathology*, 65(3), 355–356. <https://doi.org/10.1111/ppa.12486>
- Guérin-Dubrana, L., Labenne, A., Labrousse, J. C., Bastien, S., Rey, P., & Gégout-petit, A. (2013). Statistical analysis of grapevine mortality associated with esca or *Eutypa dieback* foliar expression. *Phytopathologia Mediterranea*, 52(2), 276–288.
- Guillaumie, S., Decroocq, S., Ollat, N., Delrot, S., Gomès, E., & Cookson, S. J. (2020). Dissecting the control of shoot development in grapevine: Genetics and genomics identify potential regulators. *BMC Plant Biology*, 20(1), 43. <https://doi.org/10.1186/s12870-020-2258-0>
- Hahn, P. G., & Maron, J. L. (2016). A framework for predicting intraspecific variation in plant defense. *Trends in Ecology & Evolution*, 31(8), 646–656. <https://doi.org/10.1016/j.tree.2016.05.007>
- Inch, S. A., & Ploetz, R. C. (2012). Impact of laurel wilt, caused by *Raffaelea lauricola*, on xylem function in avocado, *Persea americana*. *Forest Pathology*, 42(3), 239–245. <https://doi.org/10.1111/j.1439-0329.2011.00749.x>
- Jiménez-Díaz, R. M., Cirulli, M., Bubici, G., del Mar Jiménez-Gasco, M., Antoniou, P. P., & Tjamos, E. C. (2011). Verticillium wilt, a major threat to olive production: Current status and future prospects for its management. *Plant Disease*, 96(3), 304–329. <https://doi.org/10.1094/PDIS-06-11-0496>
- Lambert, C., Khiook, I. L. K., Lucas, S., Téléf-Micoulet, N., Mérillon, J.-M., & Cluzet, S. (2013). A faster and a stronger defense response: One of the key elements in grapevine explaining its lower level of susceptibility to esca? *Phytopathology*, 103(10), 1028–1034. <https://doi.org/10.1094/PHYTO-11-12-0305-R>
- Larignon, P., & Dubos, B. (1997). Fungi associated with esca disease in grapevine. *European Journal of Plant Pathology*, 103(2), 147–157. <https://doi.org/10.1023/A:1008638409410>
- Lauri, P.-É., Gorza, O., Cochard, H., Martinez, S., Celton, J.-M., Ripetti, V., ... Costes, E. (2011). Genetic determinism of anatomical and hydraulic traits within an apple progeny: Genetic determinism of xylem hydraulics in an apple progeny. *Plant, Cell & Environment*, 34(8), 1276–1290. <https://doi.org/10.1111/j.1365-3040.2011.02328.x>
- Lens, F., Sperry, J. S., Christman, M. A., Choat, B., Rabaey, D., & Jansen, S. (2011). Testing hypotheses that link wood anatomy to cavitation resistance and hydraulic conductivity in the genus *Acer*. *New Phytologist*, 190(3), 709–723. <https://doi.org/10.1111/j.1469-8137.2010.03518.x>
- Liebold, A. M., Brockerhoff, E. G., Kalisz, S., Nuñez, M. A., Wardle, D. A., & Wingfield, M. J. (2017). Biological invasions in forest ecosystems. *Biological Invasions*, 19(11), 3437–3458. <https://doi.org/10.1007/s10530-017-1458-5>
- Liu, M., Pan, R., & Tyree, M. T. (2018). Intra-specific relationship between vessel length and vessel diameter of four species with long-to-short species-average vessel lengths: Further validation of the computation algorithm. *Trees*, 32(1), 51–60. <https://doi.org/10.1007/s00468-017-1610-y>
- Lovisol, C., & Schubert, A. (1998). Effects of water stress on vessel size and xylem hydraulic conductivity in *Vitis vinifera* L. *Journal of Experimental Botany*, 49(321), 693–700. <https://doi.org/10.1093/jxb/49.321.693>
- Luini, E., Fleurat-Lessard, P., Rousseau, L., Roblin, G., & Berjeaud, J.-M. (2010). Inhibitory effects of polypeptides secreted by the grapevine pathogens *Phaeoconiella chlamydospora* and *Phaeoacremonium aleophilum* on plant cell activities. *Physiological and Molecular Plant Pathology*, 74(5), 403–411. <https://doi.org/10.1016/j.pmp.2010.06.007>
- Marchi, G., Roberti, S., D'Ovidio, R., Mugnai, L., & Surico, G. (2001). Pectic enzymes production by *Phaeoconiella chlamydospora*. *Phytopathologia Mediterranea*, 40, S407–S416.
- Martín, J. A., Solla, A., Esteban, L. G., de Palacios, P., & Gil, L. (2009). Bordered pit and ray morphology involvement in elm resistance to *Ophiostoma novo-ulmi*. *Canadian Journal of Forest Research*, 39(2), 420–429. <https://doi.org/10.1139/X08-183>
- Martín, J. A., Solla, A., Ruiz-Villar, M., & Gil, L. (2013). Vessel length and conductivity of *Ulmus* branches: Ontogenetic changes and relation to

- resistance to Dutch elm disease. *Trees*, 27(5), 1239–1248. <https://doi.org/10.1007/s00468-013-0872-2>
- Martínez-Diz, M. d. P., Díaz-Losada, E., Barajas, E., Ruano-Rosa, D., Andrés-Sodupe, M., & Gramaje, D. (2019). Screening of Spanish *Vitis vinifera* germplasm for resistance to *Phaeoaniella chlamydospora*. *Scientia Horticulturae*, 246, 104–109. <https://doi.org/10.1016/j.scienta.2018.10.049>
- Merdinoglu, D., Schneider, C., Prado, E., Wiedemann-Merdinoglu, S., & Mestre, P. (2018). Breeding for durable resistance to downy and powdery mildew in grapevine. *OENO One*, 52(3), 203–209. <https://doi.org/10.20870/oeno-one.2018.52.3.2116>
- Michelmore, R. W., Christopoulou, M., & Caldwell, K. S. (2013). Impacts of resistance gene genetics, function, and evolution on a durable future. *Annual Review of Phytopathology*, 51(1), 291–319. <https://doi.org/10.1146/annurev-phyto-082712-102334>
- Mondello, V., Songy, A., Battiston, E., Pinto, C., Coppin, C., Trotel-Aziz, P., ... Fontaine, F. (2017). Grapevine trunk diseases: A review of fifteen years of trials for their control with chemicals and biocontrol agents. *Plant Disease*, 102(7), 1189–1217. <https://doi.org/10.1094/PDIS-08-17-1181-FE>
- Morales-Cruz, A., Amrine, K. C. H., Blanco-Ulate, B., Lawrence, D. P., Travadon, R., Rolshausen, P. E., ... Cantu, D. (2015). Distinctive expansion of gene families associated with plant cell wall degradation, secondary metabolism, and nutrient uptake in the genomes of grapevine trunk pathogens. *BMC Genomics*, 16(1), 469. <https://doi.org/10.1186/s12864-015-1624-z>
- Morris, H., Brodersen, C., Schwarze, F. W. M. R., & Jansen, S. (2016). The parenchyma of secondary xylem and its critical role in tree defense against fungal decay in relation to the CODIT model. *Frontiers in Plant Science*, 7. <https://doi.org/10.3389/fpls.2016.01665>
- Mrad, A., Domec, J.-C., Huang, C.-W., Lens, F., & Katul, G. (2018). A network model links wood anatomy to xylem tissue hydraulic behaviour and vulnerability to cavitation. *Plant, Cell & Environment*, 41(12), 2718–2730. <https://doi.org/10.1111/pce.13415>
- Mugnai, L., Graniti, A., & Surico, G. (1999). Esca (black measles) and brown wood-streaking: Two old and elusive diseases of grapevines. *Plant Disease*, 83(5), 404–418. <https://doi.org/10.1094/PDIS.1999.83.5.404>
- Newbanks, D., Bosch, A., & Zimmermann, M. H. (1983). Evidence for xylem dysfunction by embolization in Dutch elm disease. *Phytopathology*, 73(7), 1060–1063.
- Pearce, R. B. (1996). Antimicrobial defences in the wood of living trees. *New Phytologist*, 132(2), 203–233. <https://doi.org/10.1111/j.1469-8137.1996.tb01842.x>
- Pérez-Donoso, A. G., Greve, L. C., Walton, J. H., Shackel, K. A., & Lavavitch, J. M. (2007). *Xylella fastidiosa* infection and ethylene exposure result in xylem and water movement disruption in grapevine shoots. *Plant Physiology*, 143(2), 1024–1036. <https://doi.org/10.1104/pp.106.087023>
- Pierron, R. J. G., Pouzoulet, J., Couderc, C., Judic, E., Compant, S., & Jacques, A. (2016). Variations in early response of grapevine wood depending on wound and inoculation combinations with *Phaeoacremonium aleophilum* and *Phaeoaniella chlamydospora*. *Frontiers in Plant Science*, 7. <https://doi.org/10.3389/fpls.2016.00268>
- Porth, I., White, R., Jaquish, B., & Ritland, K. (2018). Partial correlation analysis of transcriptomes helps detangle the growth and defense network in spruce. *New Phytologist*, 218(4), 1349–1359. <https://doi.org/10.1111/nph.15075>
- Pouzoulet, J., Jacques, A., Besson, X., Dayde, J., & Mailhac, N. (2013). Histopathological study of response of *Vitis vinifera* cv. Cabernet Sauvignon to bark and wood injury with and without inoculation by *Phaeoaniella chlamydospora*. *Phytopathologia Mediterranea*, 52(2), 313–323.
- Pouzoulet, J., Mailhac, N., Couderc, C., Besson, X., Daydé, J., Lummerzhim, M., & Jacques, A. (2013). A method to detect and quantify *Phaeoaniella chlamydospora* and *Phaeoacremonium aleophilum* DNA in grapevine-wood samples. *Applied Microbiology and Biotechnology*, 97(23), 10163–10175. <https://doi.org/10.1007/s00253-013-5299-6>
- Pouzoulet, J., Pivovarov, A. L., Santiago, L. S., & Rolshausen, P. E. (2014). Can vessel dimension explain tolerance toward fungal vascular wilt diseases in woody plants? Lessons from Dutch elm disease and esca disease in grapevine. *Frontiers in Plant Science*, 5. <https://doi.org/10.3389/fpls.2014.00253>
- Pouzoulet, J., Scudiero, E., Schiavon, M., & Rolshausen, P. E. (2017). Xylem vessel diameter affects the compartmentalization of the vascular pathogen *Phaeoaniella chlamydospora* in grapevine. *Frontiers in Plant Science*, 8. <https://doi.org/10.3389/fpls.2017.01442>
- Pouzoulet, J., Scudiero, E., Schiavon, M., Santiago, L. S., & Rolshausen, P. E. (2019). Modeling of xylem vessel occlusion in grapevine. *Tree Physiology*, 39, 1438–1445. <https://doi.org/10.1093/treephys/tpz036>
- R Core Team. (2019). R: A language and environment for statistical computing. (Version 3.6) [Computer software]. Retrieved from <https://www.R-project.org/>
- Riaz, S., Krivanek, A. F., Xu, K., & Walker, M. A. (2006). Refined mapping of the Pierce's disease resistance locus, PdR1, and sex on an extended genetic map of *Vitis rupestris* × *V. arizonica*. *Theoretical and Applied Genetics*, 113(7), 1317–1329. <https://doi.org/10.1007/s00122-006-0385-0>
- Rosell, J. A., Olson, M. E., & Anfodillo, T. (2017). Scaling of xylem vessel diameter with plant size: Causes, predictions, and outstanding questions. *Current Forestry Reports*, 3(1), 46–59. <https://doi.org/10.1007/s40725-017-0049-0>
- Rubio, B., Lalanne-Tisné, G., Voisin, R., Tandonnet, J. P., Portier, U., van Ghelder, C., ... Esmenjaud, D. (2020). Characterization of genetic determinants of the resistance to phylloxera, *Daktulosphaira vitifoliae*, and the dagger nematode *Xiphinema* index from muscadine background. *BMC Plant Biology*, 20, 213. <https://doi.org/10.21203/rs.2.15851/v4>
- Rusli, M. H., Idris, A. S., & Cooper, R. M. (2015). Evaluation of Malaysian oil palm progenies for susceptibility, resistance or tolerance to *Fusarium oxysporum* f. Sp. Elaeidis and defence-related gene expression in roots. *Plant Pathology*, 64(3), 638–647. <https://doi.org/10.1111/ppa.12301>
- Sabella, E., Aprile, A., Genga, A., Siciliano, T., Nutricati, E., Nicoli, F., ... Luvisi, A. (2019). Xylem cavitation susceptibility and refilling mechanisms in olive trees infected by *Xylella fastidiosa*. *Scientific Reports*, 9(1), 1–11. <https://doi.org/10.1038/s41598-019-46092-0>
- Schubert, A., Lovisolo, C., & Peterlunger, E. (1999). Shoot orientation affects vessel size, shoot hydraulic conductivity and shoot growth rate in *Vitis vinifera* L. *Plant, Cell & Environment*, 22(2), 197–204. <https://doi.org/10.1046/j.1365-3040.1999.00384.x>
- Scrucca, L. (2013). GA: A package for genetic algorithms in R. *Journal of Statistical Software*, 53(4), 1–37. <https://doi.org/10.18637/jss.v053.i04>
- Shigo, A. L. (1984). Compartmentalization: A conceptual framework for understanding how trees grow and defend themselves. *Annual Review of Phytopathology*, 22, 189–214.
- Showalter, D. N., Raffa, K. F., Sniezko, R. A., Herms, D. A., Liebhold, A. M., Smith, J. A., & Bonello, P. (2018). Strategic development of tree resistance against forest pathogen and insect invasions in defense-free space. *Frontiers in Ecology and Evolution*, 6. <https://doi.org/10.3389/fevo.2018.00124>
- Smith, H. M., Clarke, C. W., Smith, B. P., Carmody, B. M., Thomas, M. R., Clingleffer, P. R., & Powell, K. S. (2018). Genetic identification of SNP markers linked to a new grape phylloxera resistant locus in *Vitis cinerea* for marker-assisted selection. *BMC Plant Biology*, 18(1), 360. <https://doi.org/10.1186/s12870-018-1590-0>
- Sniezko, R. A., & Koch, J. (2017). Breeding trees resistant to insects and diseases: Putting theory into application. *Biological Invasions*, 19(11), 3377–3400. <https://doi.org/10.1007/s10530-017-1482-5>
- Solla, A., & Gil, L. (2002a). Xylem vessel diameter as a factor in resistance of *Ulmus minor* to *Ophiostoma novo-ulmi*. *Forest Pathology*, 32(2), 123–134. <https://doi.org/10.1046/j.1439-0329.2002.00274.x>

- Solla, A., & Gil, L. (2002b). Influence of water stress on Dutch elm disease symptoms in *Ulmus minor*. *Canadian Journal of Botany*, 80(8), 810–817. <https://doi.org/10.1139/b02-067>
- Stempien, E., Goddard, M.-L., Leva, Y., Bénard-Gellon, M., Laloue, H., Farine, S., ... Chong, J. (2018). Secreted proteins produced by fungi associated with *Botryosphaeria dieback* trigger distinct defense responses in *Vitis vinifera* and *Vitis rupestris* cells. *Protoplasma*, 255(2), 613–628. <https://doi.org/10.1007/s00709-017-1175-z>
- Stevenson, J. F., Matthews, M. A., & Rost, T. L. (2004). Grapevine susceptibility to Pierce's disease I: Relevance of hydraulic architecture. *American Journal of Enology and Viticulture*, 55(3), 228–237.
- Sun, Q., Greve, L. C., & Labavitch, J. M. (2011). Polysaccharide compositions of intervessel pit membranes contribute to Pierce's disease resistance of grapevines. *Plant Physiology*, 155(4), 1976–1987. <https://doi.org/10.1104/pp.110.168807>
- Surico, G. (2009). Towards a redefinition of the diseases within the esca complex of grapevine. *Phytopathologia Mediterranea*, 48(1), 5–10.
- Travadon, R., Baumgartner, K., Rolshausen, P. E., Gubler, W. D., Sosnowski, M. R., Lecomte, P., ... Péros, J.-P. (2012). Genetic structure of the fungal grapevine pathogen *Eutypa lata* from four continents. *Plant Pathology*, 61(1), 85–95. <https://doi.org/10.1111/j.1365-3059.2011.02496.x>
- Travadon, R., Gubler, W. D., Cadle-Davidson, L., Baumgartner, K., & Rolshausen, P. E. (2013). Susceptibility of cultivated and wild *Vitis* spp. to wood infection by fungal trunk pathogens. *Plant Disease*, 97(12), 1529–1536. <https://doi.org/10.1094/PDIS-05-13-0525-RE>
- Valtaud, C., Larignon, P., Roblin, G., & Fleurat-Lessard, P. (2009). Developmental and ultrastructural features of *Phaeoacremonium aleophilum* and *Phaeoacremonium aleophilum* in relation to xylem degradation in esca disease of the grapevine. *Journal of Plant Pathology*, 91(1), 37–51.
- Venturas, M., López, R., Martín, J. A., Gascó, A., & Gil, L. (2014). Heritability of *Ulmus minor* resistance to Dutch elm disease and its relationship to vessel size, but not to xylem vulnerability to drought. *Plant Pathology*, 63(3), 500–509. <https://doi.org/10.1111/ppa.12115>
- Venturas, M. D., Sperry, J. S., & Hacke, U. G. (2017). Plant xylem hydraulics: What we understand, current research, and future challenges. *Journal of Integrative Plant Biology*, 59(6), 356–389. <https://doi.org/10.1111/jipb.12534>
- Yadeta, K., & Thomma, B. (2013). The xylem as battleground for plant hosts and vascular wilt pathogens. *Frontiers in Plant Science*, 4. <https://doi.org/10.3389/fpls.2013.00097>

SUPPORTING INFORMATION

Additional supporting information may be found online in the Supporting Information section at the end of this article.

How to cite this article: Pouzoulet J, Rolshausen PE, Charbois R, et al. Behind the curtain of the compartmentalization process: Exploring how xylem vessel diameter impacts vascular pathogen resistance. *Plant Cell Environ*. 2020;43:2782–2796. <https://doi.org/10.1111/pce.13848>